

AEROSOL RADIATIVE FORCING AND MODEL RESPONSES

V. Ramaswamy

Atmospheric and Oceanic Sciences Program

Princeton University

Princeton, New Jersey 08540, USA

ABSTRACT

The effects on the surface-atmosphere system due to aerosols are surveyed, with an emphasis on the radiative aspects of aerosols generated by noncatastrophic, nonepisodic events. Solar absorption and scattering by one type of "nominal" tropospheric aerosols is chosen as an example to illustrate the nature of the perturbations in the radiative fluxes at the surface, at the top of atmosphere, and in the atmospheric layers. The range in the magnitude of the perturbations can be quite large when catastrophic or episodic events are also considered. The effects of the aerosol perturbations in the solar spectrum are analyzed by considering the compensation effects due to radiative and radiative-convective mechanisms. These constitute idealistic atmospheric responses, wherein all the mechanisms are confined in a local vertical column and changes in the hydrologic cycle are ignored. Estimates of these responses are compared with those reported from global three-dimensional general circulation model simulations. The results suggest that an aerosol-induced radiative forcing can cause changes in the local energy balance and in the circulation, besides causing changes in the atmospheric thermal profile.

The coupling of the aerosol microphysics and radiative and dynamical mechanisms has been achieved thus far only in the study of catastrophic and episodic events. Future investigations would need to focus more on these aspects for all types of aerosols. Robust estimates of the sources and optical properties as well as a better understanding of the microphysical and transport processes are needed to assess the aerosol-induced radiative-dynamical-microphysical interactions unambiguously.

1. INTRODUCTION

The extent to which aerosols interact with and/or modify the general circulation of the atmosphere and climate has been addressed by the use of models of varying complexity. These include one- and two-dimensional models of the energy balance and radiative-convective types, limited-area and mesoscale models and, ultimately, completing the hierarchy, the three-dimensional global general circulation models (GCMs). A general perspective on the methodology and results of model studies can be had from the collection of papers in Gerber and Deepak

(1984) and the Proceedings of the 1984 International Radiation Symposium (Fiocco, 1984).

The typical atmospheric aerosol (radii $> 0.001 \mu\text{m}$) is a heterogeneous entity comprised of several different components. By virtue of its size, shape, and composition, the aerosol is capable of exerting chemical and physical effects. The aerosol forcing on the atmosphere can be classified as: 1) microphysical forcing involving the transformation (including cloud drop nucleation, coalescence, aggregation, etc.) and removal of the aerosol, and 2) radiative forcing involving the scattering and absorbing of radiation. An initial microphysical forcing may eventually lead to a radiative forcing, e.g., formation of clouds. Both types of forcing can perturb the atmospheric energy budget and, thus, the climate.

Since there already exists a collection of recent research work on aerosol-related issues, as referenced earlier, a narrower aspect of the subject constitutes the focus of this review. More specifically, this review concerns itself with the general nature of the aerosol radiative forcing and the assessments of the response to this forcing. The discussions are presented with some particular numerical examples; some recent investigations into the various aspects of the subject are also mentioned, although these are necessarily limited and brief.

The radiative forcing, in general, depends on the aerosol optical properties, their vertical distribution, solar zenith angle, and presence of other scatterers (surface clouds and gas molecules; see Ackerman, 1987). Owing to the temporal and spatial variations in aerosol properties, it is not an easy task to formulate the precise nature of the aerosol radiative forcing. The lack of knowledge of the global distribution of aerosol characteristics has meant that assumptions have to be made in estimating the aerosol-induced forcing. This is unlike the more precisely defined radiative forcing of well-mixed, homogeneously distributed species, such as carbon dioxide.

The nature of the aerosol radiative perturbations is discussed first. To illustrate this point, a sensitivity study is performed with respect to one characteristic of the aerosols, namely, their absorptivity in the visible spectrum. For this purpose, "nominal" tropospheric aerosols with a scale-height dependence and located above a low albedo surface are assumed. "Nominal" here implies aerosols arising due to noncatastrophic, nonepisodic processes; mixtures of aerosols with water drops are also excluded. The range of the perturbations for various types of aerosols are also reviewed.

The response of the atmosphere to a "nominal" aerosol radiative forcing is discussed next. From a theoretical standpoint, the response to the perturbations in the radiative fluxes can involve, in ascending order of complexity, purely radiative or radiative-convective or radiative-convective-dynamical responses. A one-dimensional and a three-dimensional model are considered to investigate the change in the atmospheric temperatures and the readjustment of the energy budget. In the present text, the response of the one-dimensional model

is derived on the basis of two different but idealistic assumptions: these are, respectively, the radiative (wherein radiative processes alone compensate for the perturbation) and the radiative-convective (wherein radiative and convective processes compensate for the perturbation) solutions. For the radiative response solution, aerosol perturbation (absorption) is assumed only for a particular layer while, for the radiative-convective response solutions, a purely absorbing or a purely scattering aerosol is assumed whose forcing occurs throughout the atmospheric column. Results arising out of these two different assumptions are then compared with the response from a GCM experiment performed by Coakley and Cess (1985). The comparison highlights the relative roles played by the radiative and the nonradiative components of the energy budget in the one-dimensional and the three-dimensional models, respectively. Results from other GCM studies that illustrate the nature of the model atmosphere response to aerosol perturbations are also surveyed. The various GCM studies serve to identify the mechanisms that are important in different regions of the atmosphere and for various types of aerosol radiative forcing.

Finally, the direction in which the aerosol-related modeling efforts are proceeding is surveyed; some of the studies that have coupled aerosol microphysical and radiative processes are mentioned. Problems in the determination of the aerosol-related effects, that are unsolved or whose solutions remain considerably uncertain, are stated at the end.

2. AEROSOL RADIATIVE FORCING

There are three ways in which aerosols can exercise a radiative perturbation to an atmosphere in radiative-convective-dynamical equilibrium:

- 1) change the absorption or emission of radiation at the levels where they occur in the atmosphere (Deepak and Gerber, 1984),
- 2) alter the radiative fluxes at levels other than where the aerosols occur (Deepak and Gerber and references therein) and
- 3) alter the optical properties of the atmosphere through interaction with water vapor, e.g., formation of haze drops, external or internal mixtures with cloud drops. (Twomey, 1976, Chylek et al., 1984, Charlson et al., 1987, Coakley et al., 1987).

The radiative influences can occur in both the solar and the longwave spectrum (Carlson and Benjamin, 1980; Grassl, 1987; Pollack and Ackerman (1983)). For the commonly occurring submicrometer aerosols, however, the principal influence is in the solar spectrum. Based on our present knowledge of optical properties (Shettle and Fenn, 1979), most aerosols scatter in both the visible and the near-infrared spectrum while absorbing only in the near-infrared spectrum. Graphitic carbon and particles derived from iron oxides possess absorption bands in the visible as well.

An example is given to illustrate the general nature of the aerosol-induced radiative forcing. A 1-km-scale height profile for the aerosol number concentration is assumed; the aerosol sizes are lognormally distributed (mode radius is $0.1 \mu\text{m}$, standard deviation is 2), with refractive indices in the near infrared as given by Shettle and Fenn (1979) for water soluble aerosols. In the visible, the refractive index is assumed to be a variable. The aerosol single scattering parameters are employed in a one-dimensional radiative transfer model (Ramaswamy and Kiehl, 1985) of the clear tropical atmosphere. The cosine of the solar zenith angle is taken to be 0.6, the surface albedo is 0.07 (representative of oceans), and the calculations are performed for diurnally averaged conditions. The aerosol optical depth at a wavelength of $0.5 \mu\text{m}$ is assumed to be 0.1.

The aim is to examine the changes in the solar heating rate and the changes in the shortwave fluxes at the atmospheric boundaries (viz., top of atmosphere and surface) due to changes in the visible spectrum characteristics of the aerosols (e.g., due to presence of carbonaceous compounds or iron oxides). Specifically, changes in the imaginary part of the refractive index in the visible spectrum ($\text{Im}(m)$) are considered, while the real part is held fixed: these are, respectively, $\text{Im}(m)$ of 0 (mildly absorbing, i.e., absorbing only in the near infrared), 0.01 (moderately absorbing), and 0.1 (strongly absorbing). It may be noted that these values are within the range measured at rural and urban locations.

The solar heating rate in the clear tropical lower atmosphere (0-6 km.) is shown in Fig. 1a (layers are 1 km thick). The heating increases with decreasing altitude, owing to the increase in water vapor concentration and the water vapor absorption bands in the near infrared. The changes in these heating rates when aerosols are introduced into the surface-atmosphere system are shown in Fig. 1b. Due to the assumed aerosol vertical profile, the strongest perturbations occur in the lower troposphere. For the mildly absorbing aerosol, the increase is $< 0.1 \text{ K/d}$; - and this is due solely to the aerosol characteristics in the near infrared. The perturbation increases with $\text{Im}(m)$ and a value of up to 0.5 K/d is attained for an $\text{Im}(m)$ of 0.1. While the difference in absorption between the mildly absorbing and the clear sky cases is a consequence of near-infrared aerosol characteristics, that between the various aerosol cases is due to the properties in the visible spectrum.

The changes in the fluxes at the top of the atmosphere and at the surface for the three aerosol cases are listed in Table 1. Also listed are the absolute values of the fluxes for the clear sky case and the value of the single scattering albedo at a wavelength of $0.5 \mu\text{m}$. Increasing $\text{Im}(m)$ decreases the value of the single-scattering albedo, resulting in increasing flux convergence in the atmosphere. Correspondingly, the flux at the surface decreases monotonically. The reflected flux at the top of the atmosphere increases with respect to the clear sky value for the mildly absorbing case; this is because the presence of the aerosols increases the backscattering. With an

TROPICAL ATMOSPHERE

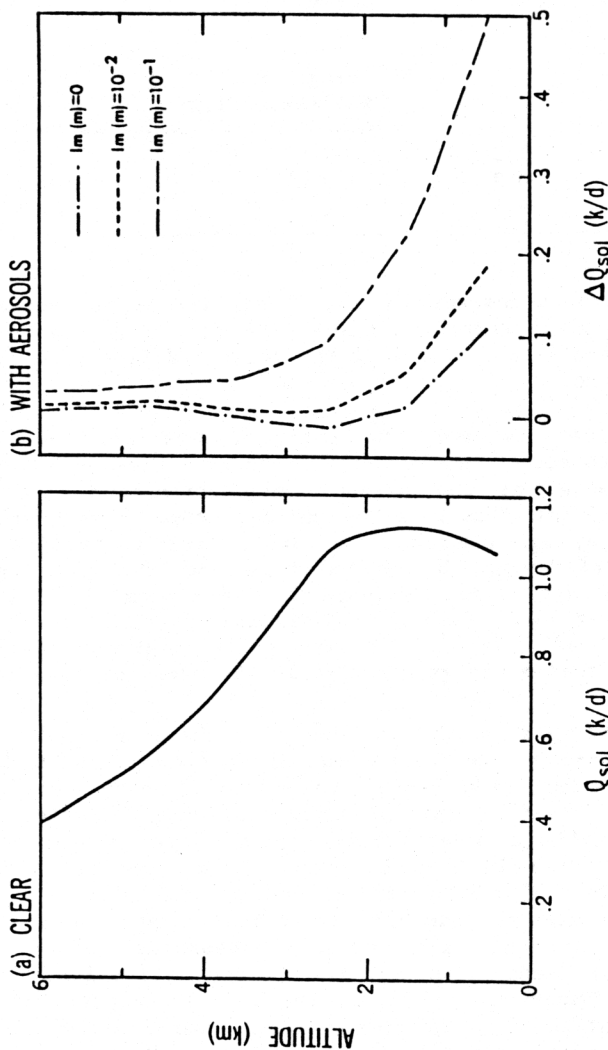


FIGURE 1. a) Solar heating rate, Q_{sol} (in degrees per day), in a diurnally-averaged clear tropical atmosphere (McClatchey et al., 1972) and b) change in the solar heating rate, ΔQ_{sol} , due to aerosols with different values of the imaginary part of refractive index, $Im(m)$, in the visible spectrum. The values chosen are 0 (i.e., nonabsorbing in the visible), 0.01 (moderately absorbing), and 0.1 (strongly absorbing), respectively.

TABLE 1. AEROSOL OPTICAL PROPERTIES AND BOUNDARY FLUXES

Aerosol Absorption	Im(m)	ω	Reflected Flux (W/m^2)	Surface Flux (W/m^2)
CLEAR	-	-	41.9	322.8
			Change in Reflected Flux	Change in Surface Flux
Mild	0	1.0	+ 3.4	- 7.3
Moderate	0.01	0.7	+ 3.0	- 8.5
Strong	0.10	0.6	- 0.2	-15.0

increase in the aerosol absorption, the change in the reflected flux becomes less (moderately absorbing case). In fact, for the strongly absorbing case, there is a decrease in the reflected flux with respect to the clear sky case.

For the conditions assumed, the surface always loses some solar flux. The atmosphere may or may not experience an increased solar flux convergence depending on the aerosol absorption and scattering characteristics. The net flux into the surface-troposphere system can increase or decrease, again depending on the aerosol properties. This feature of loss of energy by the surface and the gain by the surface-troposphere system is discussed in the context of absorbing aerosols by Cess et al. (1985). McCracken et al. (1986) have studied the case of aerosols in the polar regions where the surface-atmosphere system can gain energy in the presence of aerosols.

The foregoing example is just one aspect of the sensitivity of the aerosol radiative forcing. As pointed out in Section 1, the magnitude of the radiative perturbation depends on several factors. We discuss them below briefly based on earlier investigations. Coakley et al. (1983) show that while a nonabsorbing aerosol layer (optical depth 0.1) causes an increase in the planetary albedo over all types of surfaces, a moderately absorbing aerosol reduces the planetary albedo for surface albedos greater than 0.3. Their study also reveals that a decrease in solar zenith angle for a nonabsorbing aerosol layer (optical depth 1.0) leads to a decrease in the reflectivity of the layer. As shown by Ramaswamy and Kiehl (1985) in the context of smoke aerosols, the distribution of the heating perturbation in the atmosphere depends on the aerosol vertical profile.

A summary of the maximum heating rate perturbations that have been reported in the literature for various aerosol types (either based on model assumptions or observations) is presented in Table 2. These values may be compared with the clear tropical sky heating due to water vapor absorption (1.1 K/d at 0.5 km.; see Fig. 1a). Also listed are the altitudes of the assumed perturbation. The layer thicknesses,

TABLE 2. MAXIMUM PERTURBATION HEATING RATES
(SOLAR) FOR VARIOUS AEROSOL TYPES

Aerosol Type	Perturbation (K/d)	Altitude (Km)	Source
1 km. Scale Height	0.5	0.5	This study
Desert Dust	4.0 7.0	3.5 1.0	Carlson and Benjamin (1980); Fouquart et al. (1984)
Arctic Haze	0.4 1.1	5.5 0.8	Blanchet and List (1984); Valero et al. (1984)
Volcanic	0.1	28.0	Valero et al. (1984)
Water/Ice Cloud	> 1	Troposphere	Ramaswamy and Kiehl (1985)
Nuclear War	> 5	Troposphere	Ramaswamy and Kiehl (1985)

the averaging period, and the geographical locations considered vary for the different investigations (the intent here is to merely point out the range). The wide range of values emerging from this tabulation is a measure of the possible extent of the aerosol forcing in the Earth's atmosphere. It also points out the difficulty of formulating a global forcing that would incorporate the different types of aerosols, since each type has its own distinct signature. Toon and Pollack (1976) and Deepak and Gerber (1983) present unified models that present the average aerosol properties under nominal, non-catastrophic circumstances. One characteristic involving the aerosols, not categorised in Table 2, which is manifested in cloud optical properties, is the effect of aerosols present as external or internal mixtures with water drops or ice crystals. This perturbation can be substantially higher than that posed by the dry aerosol alone (Chylek et al., 1984; Coakley et al., 1987).

A summary can also be made about the aerosol-induced perturbations in the solar fluxes at the boundaries of the atmosphere. In this case, too, the range of possible values is large; the depletion of the flux at the surface can range from small values (few W/m^2 for background

tropospheric aerosol) through moderate values (e.g., 10-50 W/m² for desert duststorms) to extreme values (e.g., 150 W/m² for catastrophic events). The change in the net solar flux at the top of the atmosphere can range from small negative values (for scattering aerosols) to very high positive values (for large loadings of absorbing aerosols).

The extremities in the aerosol radiative forcing imply that there would be a large variability in the surface-atmosphere response for different aerosol types. This is indeed borne out by comparing the GCM simulations of "nominal" tropospheric aerosol effects (Coakley and Cess, 1985; Geleyn and Tanre, 1984) with the GCM simulations of catastrophic aerosol effects (Covey et al., 1984; Malone et al., 1986).

Returning to the focus in this paper on the "nominal" aerosol forcing, the response to such a forcing is evaluated next. Before beginning this investigation and as a final point to the present section, the study by Coakley and Cess (1985) is cited to illustrate a global model of the background aerosol solar radiative forcing (diurnal averages for July conditions). This is shown in Fig. 2 as 1) change in the radiative flux at the top of the atmosphere, 2) change in the radiative flux at the surface, and 3) change in the atmospheric solar heating rate. In this particular study, the aerosol scattering dominates the absorption; the nature of the forcing at all latitudes involves changes as discussed earlier. The globally-averaged change at the top of the atmosphere is -3.5 W/m² and that at the surface -5.0 W/m², so that the increase in the atmospheric absorption is 1.5 W/m². The GCM response to this forcing will be discussed in Section 4.

3. RADIATIVE AND RADIATIVE-CONVECTIVE RESPONSES

The response of the surface-atmosphere system to the aerosol perturbations is investigated first using a one-dimensional model and by making some simple assumptions about the atmospheric physical processes. For an atmosphere in radiative-convective-dynamical equilibrium, the rate of change of temperature at any level is given by

$$\frac{dT}{dt} = Q_{sol} + Q_{lw} + Q_{conv} + Q_{dyn} = 0 \quad (1)$$

where Q_{sol} , Q_{lw} , Q_{conv} and Q_{dyn} denote, respectively, the heating due to solar, longwave, convective, and dynamical processes. The convective heating is the sum of the sensible and latent heat while the dynamical heating is the sum of diffusion, and mean and eddy circulations.

3.1 RADIATIVE RESPONSES

Consider the response of the atmosphere when both convective and dynamical heating are assumed to be fixed, i.e., Q_{conv} and Q_{dyn} are

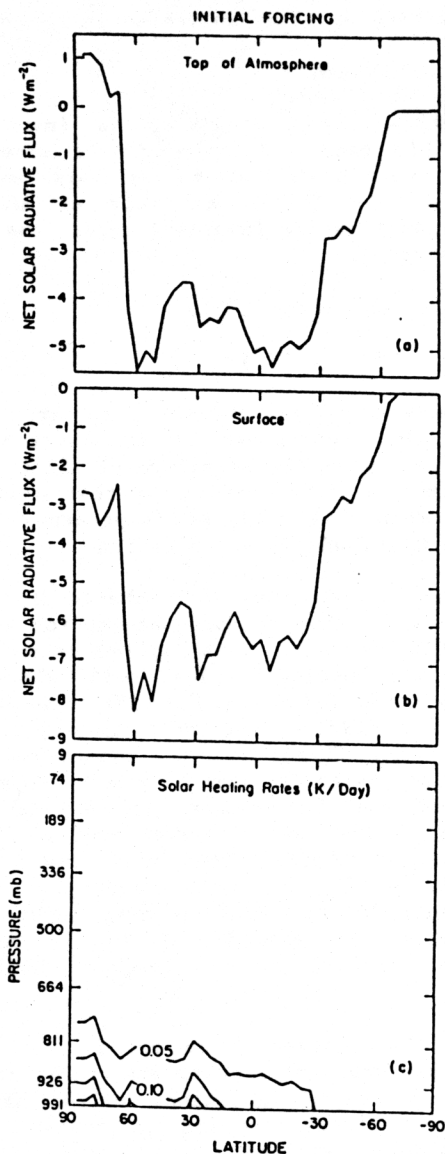


FIGURE 2. Zonally-averaged solar radiative forcing due to the background tropospheric aerosol illustrates: a) change in the net solar flux at the top of the atmosphere, b) change at the surface and c) change in the solar heating (degrees per day). (From Coakley and Cess, 1985.)

unaltered by the perturbation. Then, if the aerosol-induced increase in solar heating is ϵ and Δ denotes the change in the quantities, the response to this heating would be an increased longwave cooling, i.e.,

$$\Delta Q_{lw} = -\epsilon \quad (2)$$

Both the perturbation and the response involve the radiative processes only in this case. Equation (3) is essentially the fixed dynamical heating concept introduced by Fels and Kaplan (1976), Ramanathan and Dickinson (1979) and Fels et al. (1980). For an atmosphere whose properties are invariant across the longwave spectrum (i.e., "gray" atmosphere),

$$\Delta Q_{lw} \propto (-\Delta(T^4)), \quad (3)$$

hence,

$$\Delta T \propto (\epsilon/4T^3)$$

Thus, under this assumption, the result of an aerosol-induced heating is an increase in the temperature of the layer where the heating occurs. It is also seen that the magnitude of the temperature response increases with decreasing temperature so that upper levels in the troposphere would experience a higher temperature change than lower levels for the same magnitude of perturbation.

Numerical values of the temperature change in the clear tropical atmosphere under the radiative response assumption are calculated when a perturbation heating of 0.2 K/d is applied to any layer (note from Table 2 that this is a "nominal" value, well below the upper end of the range). This is performed using the radiative-convective model of Ramaswamy and Kiehl (1985) and the McClatchey (1972) tropical atmosphere profile with fixed surface temperature and fixed water vapor profile. The rationale for fixed surface temperature arises out of consideration of the large heat capacity of the oceans. The rationale for the static water vapor profile is to avoid the complicated feedback effects involving the hydrologic cycle (Ramanathan, 1981), which are not adequately represented in a one-dimensional model. In the simulations to be described below, the sum of the convective and dynamic heating is assumed to be the negative of the net radiative (solar + longwave) heating, according to Eq. (1).

Three layers in the troposphere and one in the stratosphere are considered for the perturbation experiments; these are listed in Table 3 (note that the layer configurations differ from that used to describe the aerosol radiative forcing in Section 2). Four different simulations are performed, with each layer being perturbed in turn. In each simulation, the solar heating rate is increased by 0.2 K/d in the layer under consideration. Then, the temperature profile of the model atmosphere is time-marched to a new equilibrium solution, with the longwave radiative process responding to the imposed perturbation, such that the condition given by Eq. (1) is established again. For the numerical solutions, equilibrium is deemed to occur when the left-hand side of Eq. (1) is less than 0.001 K/d. The resulting temperature

TABLE 3. LAYER SPECIFICATIONS, HEATING PERTURBATION, AND CORRESPONDING FLUX PERTURBATIONS FOR THE RADIATIVE AND RADIATIVE-CONVECTIVE RESPONSE EXPERIMENTS

Perturbed Layer Location (Km)	Heating Perturbation (K/d)	Flux Perturbation (W/m ²)
0.1 - 0.5	0.2	0.7
3.0 - 4.2	0.2	2.1
7.2 - 9.2	0.2	2.0
19.4 - 21.3	0.2	0.1

change in the four different simulations for the four specific layers are listed in Table 4. Although the magnitude of the perturbation chosen is arbitrary, it is within the range that can be encountered in noncatastrophic situations. As will be seen later, were the three-dimensional model to respond in this manner, the magnitude of the temperature response, as obtained from the experiments in this section, would be well above the normal variability.

The radiative response can be expected to hold in the stratosphere where the atmosphere tends to be in radiative equilibrium on an annual basis (Ramanathan and Dickinson, 1979; Fels et al. 1980). By analogy, the radiative responses derived here should be regarded as limiting temperature changes that occur only when radiative processes are important for the compensation. In the troposphere, however, convective processes play a major role in distributing heat energy and, with the possible exception of the upper troposphere, it is not justified to assume fixed convective heating. Hence, it is more meaningful to consider the radiative-convective response of the troposphere to an aerosol radiative forcing.

TABLE 4. CHANGE IN THE RADIATIVE RESPONSE TEMPERATURE OF THE LAYER DUE TO AN AEROSOL-INDUCED INCREASE IN THE SOLAR HEATING RATE.

Perturbed Layer Location (Km)	ΔT (Perturbed Layer) (K)
0.1 - 0.5	0.31
3.0 - 4.2	0.97
7.2 - 9.2	1.58
19.4 - 21.3	1.97

3.2 RADIATIVE-CONVECTIVE RESPONSES

The radiative-convective response is evaluated by parameterizing the convective heat transfer as a diffusive process (see Ramaswamy and Kiehl, 1985); in this formulation, the convective flux exchange between two adjacent layers is linearly related to the temperature gradient. Surface fluxes follow the prescription of Ramanathan (1981). A critical lapse rate of 6.5 K/km is assumed for the simulations in this section. The McClatchey (1972) tropical atmosphere profile is again taken as the initial equilibrium profile.

As before, the heating perturbation is applied to each of the four layers individually. It is assumed first that the aerosol is absorbing only. Further, in order to simulate the reduction in solar flux below the perturbed layer (owing to aerosol absorption in the layer), the net solar flux below the layer is reduced by an amount equal to that absorbed by the layer. The amount of flux absorbed, corresponding to each of the four layers, is listed in Table 3. The simulations for the radiative-convective response solution are in contrast to the simulations for the radiative response solution where the heating of the layer was the only perturbation; in the present case, less solar flux is incident on the layers below the perturbed layer. As before, the surface temperature and the water vapor profile are held fixed.

For the simulations in this section, since convective heating is calculated explicitly, the dynamical heating is assumed to be the negative of the sum of the convective and the net radiative heating, again according to Eq. (1). The solar flux perturbation is applied according to the details in the preceding paragraph and the temperature profile is time-marched to a new equilibrium solution. In contrast to the previous section, the assumptions in this section allow both the radiative and the convective mechanisms to participate in the compensation process. For the numerical solutions, equilibrium requires, besides the heating rate criterion mentioned in Section 3.1, the additional constraint that the lapse rate be less than the critical lapse rate everywhere in the column.

The magnitude of the change in the temperature in the case of perturbation in each of the four layers is listed in Table 5. The changes are less than for the radiative response experiments. This can be explained as follows. Analogous to Eq. (2), the new balance in the heating rate in the concerned layer can be written as

$$\Delta Q_{lw} + \Delta Q_{conv} = -\epsilon \quad (4)$$

In contrast to Section 3.1, there are now two readjustment mechanisms to compensate for the heating perturbation in the layer. The presence of convective heat transport diminishes the influence of the longwave adjustment and leads, thus, to a lesser increase in temperature. For the layers below the perturbed layer, the decrease in flux necessitates a readjustment whereby the temperature is reduced (the balance equations for the layers below are similar to Eq. (4)). The cooling below the perturbed layer is illustrated by the decreases in the surface-air temperature, as listed in Table 5.

TABLE 5. CHANGE IN THE RADIATIVE-CONVECTIVE RESPONSE TEMPERATURE (ΔT (LAYER)) DUE TO AN AEROSOL-INDUCED PERTURBATION

Layer (Km)	A b s o r p t i o n		S c a t t e r i n g	
	ΔT (K)	ΔT (K)	ΔT (K)	ΔT (K)
	(layer)	(surface)	(layer)	(surface)
0.1-0.5	0.08	-0.20	-0.51	-1.07
3.0-4.2	0.17	-2.13	-0.69	-1.71
7.2-9.2	0.67	-2.28	-0.17	-2.85
19.4-21.3	2.32	-0.26	-0.02	-0.03

Another comparison can be made with the radiative response solutions. The heating in any layer, unaccompanied by flux changes in layers below (as in the radiative response experiments in Section 3.1) leads to, by virtue of the longwave radiation, increased longwave flux convergence in other layers as well. This, in turn, gives rise to an additional longwave flux convergence in the layer that was perturbed directly. When the solar flux decreases in the layers below the perturbed layer (which occurs for the experiments in this subsection), there is a cooling below that counteracts the increased radiating effect of the perturbed layer. Thus, the net change in the temperature at any layer is dependent on the redistribution by the longwave radiative exchanges in the column.

Finally, the radiative-convective response when the aerosols are assumed to be nonabsorbing is considered; the perturbation in this case is one of a reduction of solar flux in the entire surface-atmosphere system, including the layers considered in Table 3. Here, the aerosol absorption is ignored and the solar flux in the entire column is depleted by an amount corresponding to a heating of 0.2 K/d. Again, the same four layers are considered individually and four simulations are performed. The magnitude of the changes in temperature are also listed in Table 3. As should be expected, the entire column cools; this is indicated by the decrease in temperature in the layer where heating was applied in the foregoing cases, and in the surface-air layer.

The conclusions to be drawn from the radiative-convective experiments are that while aerosol-induced solar absorption tends to increase the temperature of the entire column, the aerosol-induced scattering tends to cool the column. The net effect at any level in the column is a function of the degree of the aerosol absorption-to-scattering. The longwave radiative effects are felt throughout the column. Convective heat transfer, as modeled here on the assumption of a diffusive mechanism, competes with the longwave radiation and tends to limit the temperature response, especially when compared with the predictions from the radiative response solutions.

The only regions where the convective processes would not be directly effective in the compensating process would be the lower stratosphere and above (although indirect effects due to changes in the troposphere cannot be ruled out).

Two major points, which are beyond the focus of simple models and whose effects cannot be gauged by experiments with the one-dimensional model used in this section, concern the hydrologic cycle and the nature of the large-scale dynamical adjustments. The former is crucial not only for the longwave radiative changes but also for the latent heat adjustments. Both the moisture-related effects and the large-scale dynamics require the numerical solution to the primitive equations and their response can be properly addressed only with the three-dimensional general circulation models. As seen in the next section, important physical adjustments occur in GCMs, all of which cannot be anticipated by the radiative and the radiative-convective response experiments performed here.

4. GENERAL CIRCULATION MODEL RESPONSES

The GCM experiments reported in the literature have addressed the problem of either small perturbations such as those arising due to tropospheric and stratospheric aerosols (Coakley and Cess, 1985; Geleyn and Tanre, 1984; Tanre and Geleyn, 1984) or large perturbations following catastrophic events (Covey et al., 1984). Here, we focus mainly on the small perturbations due to tropospheric aerosols; we will mention some of the results concerning other types of aerosols at the end of the section.

Coakley and Cess (1985) have studied the response of the National Center for Atmospheric Research General Circulation Model (called the Community Climate Model or CCM) to the forcing shown in Fig. 2 and which was described in Section 2. The aerosol-induced changes in the Northern Hemisphere mean temperature profile (July conditions) from their GCM simulation with fixed sea-surface temperature is shown in Fig. 3. Also shown in that figure by the gray shading is the normal variability of the model. The GCM response was below the normal variability of the model at any level in the troposphere. It would appear that the cooling in the troposphere (Fig. 3) is the result of the aerosol scattering dominating over its absorption. While this would be consistent with the radiative-convective response solution for the scattering only case (Section 3.2), there is a more logical reason for the GCM behaviour.

The explanation can be had from Coakley and Cess' (1985) examination of the energy balance between the physical processes in the control and the perturbed cases. They analyzed the North African region in this connection and this is illustrated in Fig. 4. The control in Fig. 4a shows the tropospheric values of the net radiative heating rate (sum of solar and longwave), Q_{rad} , the convective heating, Q_{conv} , the dynamical heating, Q_{dyn} , and the heating due to large-scale ascending motions, Q_w . There is a balance essentially

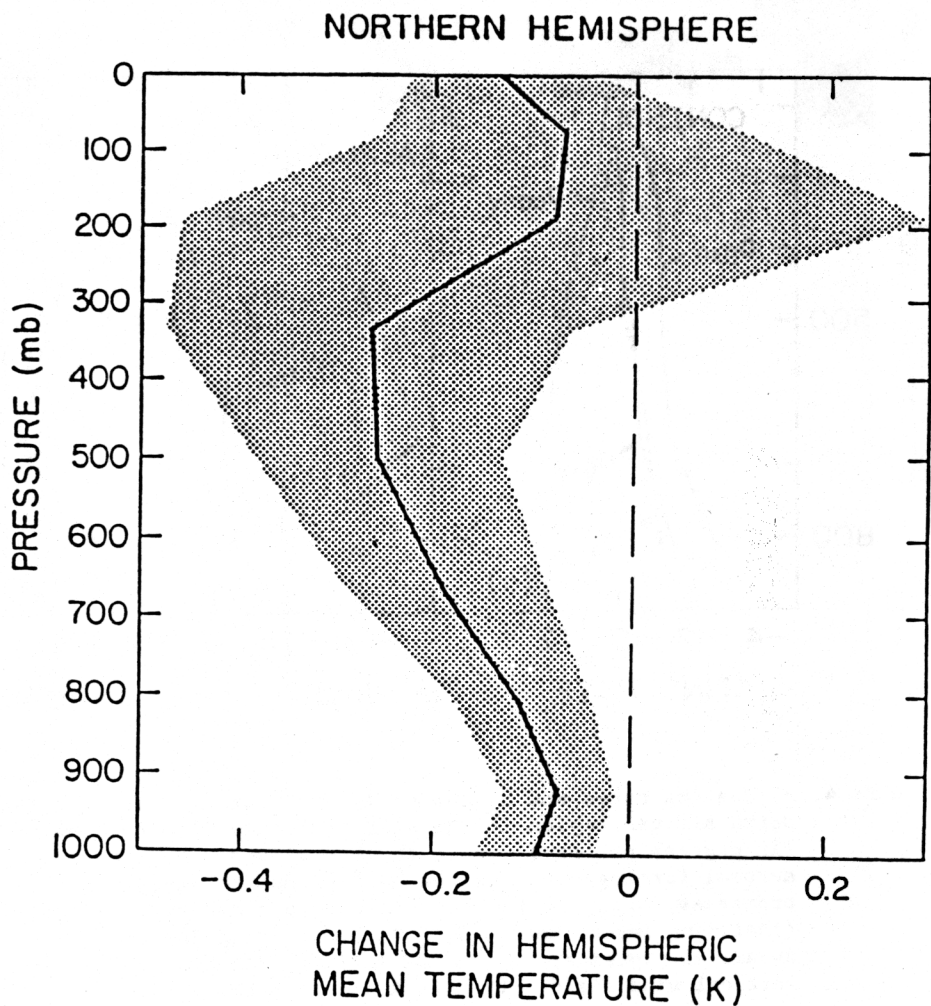


FIGURE 3. Change in the Northern Hemisphere mean temperature of the NCAR Community Climate Model due to the aerosol forcing shown in Figure 2. The gray area represents the "noise" level of the model. (From Coakley and Cess, 1985.)

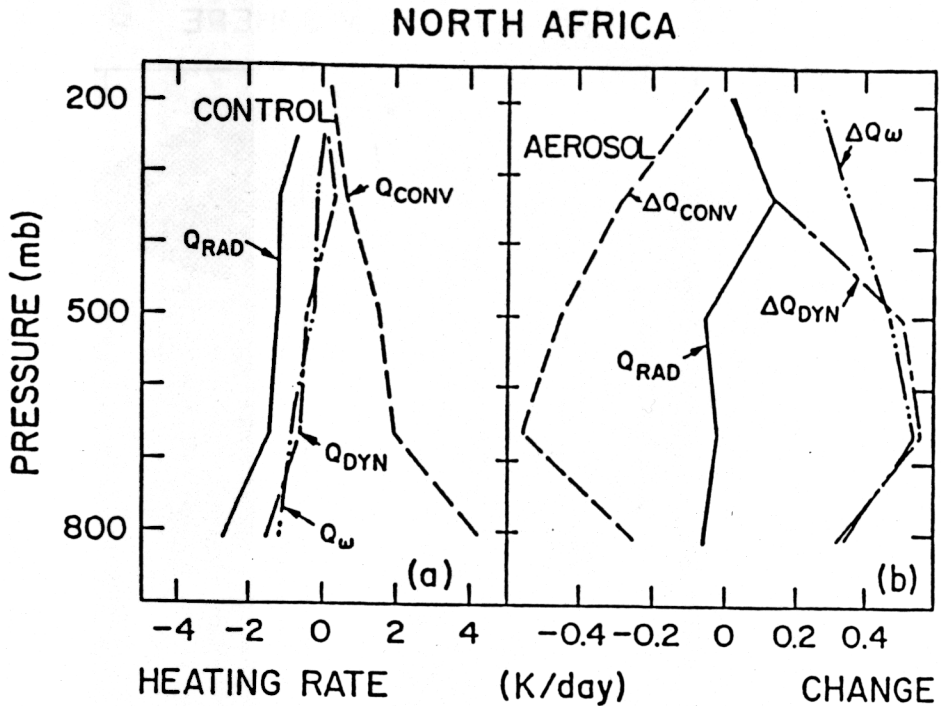


FIGURE 4. a) Heating rates and b) change in the heating rates for the North African region in the NCAR Community Climate Model (in degrees per day) due to the background tropospheric aerosol forcing. Q_{rad} is the heating due to radiative processes, Q_{conv} is the heating due to convective processes (including latent heat), Q_{rad} is the heating due to dynamical processes. Q_w is the heating rate due to the vertical wind field. (From Coakley and Cess, 1985.)

between the radiative cooling and the convective heating. The dynamical cooling term is small and nearly all of this is supplied by the uplift. There is a low-level convergence in this region and moisture is transported upwards by the vertical wind field. Condensation and latent heat release follow. In the perturbed situation (the changes in the heating rates with respect to the control case are shown in Fig. 4(b)), the reduction of the solar flux absorbed at the surface leads to a cooling and a decrease in the surface fluxes of sensible and latent heat. Convection is suppressed and ΔQ_{conv} is negative. Radiative cooling undergoes little change in the lower troposphere while there is a small decrease in the upper troposphere. Note that this is in contrast to the increase in the cooling of the column obtained for the radiative-convective response (scattering only case) in Section 3.2.

Since changes in Q_{conv} are larger in magnitude relative to the changes in Q_{rad} and because of the balance between the radiative and convective terms in the control (Fig. 4(a)), one may have expected the suppression of convective activity in the perturbed case to lead to a cooling throughout the troposphere. However, the decrease in tropospheric diabatic heating ($Q_{\text{conv}} + Q_{\text{rad}}$) led to changes in the circulation. This resulted in a decrease in the dynamical cooling, thus offsetting the reduction in convective heating. Thus, the magnitude of the change in the temperature remained small everywhere (Fig. 4) and within the noise levels of the model. The value of Q_w indicates that the dynamical changes were brought about primarily by a reduction in the vertical velocity (less adiabatic cooling). While the control case had an excess of precipitation over evaporation, the perturbed case had the two processes nearly in balance. There was also a decrease in cloudiness over this region. Other geographical regions also underwent cooling in the troposphere. For all the other regions, although it was possible to state in general terms that the reduction in the solar flux at the surface had reduced convection, the small changes in the terms did not permit an easy identification of the precise mechanisms.

Summarising, the GCM response, with fixed sea-surface temperatures, being controlled by moist convective processes in the Northern Hemisphere, led to small temperature changes throughout the column. The temperature response was primarily due to a suppression of the convective activity brought about by the reduction of solar flux at the continental surfaces. The dynamic response was limited to changes in vertical velocity. Thus, in assessing the response to an aerosol radiative forcing, the GCM results indicate that it is important to consider the effects of changes in the hydrologic cycle, convective heat transfer, and large-scale dynamics, although the magnitudes involved may be insignificant for "nominal" aerosol optical depths. Recalling the responses of the column models (Section 3), although the sign of the temperature changes obtained there does correspond to those obtained in the GCM, the magnitudes differ owing to the presence of nonradiative feedback mechanisms in the GCMs. It is, of course, yet to be verified whether the feedbacks occurring in the GCM simulations are similar in scale and magnitude to those

occurring in the actual atmosphere. The GCM results also suggest that large local temperatures are not likely to occur for small perturbations involving predominantly scattering aerosols. Land surface temperature responses are likely to remain small if ocean surface temperatures are fixed, unlike the results from radiative-convective models with land surfaces of zero heat capacity. It may be noted again that this GCM study employed fixed sea-surface temperatures. The consequence of an explicit formulation of atmosphere-ocean interactions in GCMs on the aerosol-related impacts is yet to be investigated.

This section is concluded by discussing other experiments with GCMs that have employed different aerosol forcings. Geleyn and Tanre (1984), using the European Center (ECMWF) GCM, employed seven different aerosol models to estimate the short-term climatic response. They, too found that the compensation to the tropospheric aerosol forcing involved nonradiative effects. There was no detectable temperature response except above midtropospheric levels. An interesting result from their experiments was the large land surface coolings (3 K) in the Sahara due to a large desert aerosol optical depth and its vertical distribution.

Tanre and Geleyn (1984) also carried out a simulation of a stratospheric aerosol perturbation similar to that from El Chichon. For a globally-averaged optical depth of 0.15, a 1-3 K increase resulted in the stratospheric temperature at 30 mb (0-35 N). The temperature changes occur due to solar and longwave aerosol properties. Pitari et al. (1987) have also deduced temperature increases using a residual eddy circulation model of the stratosphere. It is important to point out that Pollack and Ackerman (1983) have estimated similar temperature changes using a radiative-convective model. Thus, the solutions from the radiative and the radiative-convective responses described in Section 3.2 are probably applicable in sign and, perhaps, even in magnitude, to aerosol-induced heating perturbations near the lower stratosphere. It may be noted from Tables 4 and 5 that in both the radiative and radiative-convective solutions, the layer situated near 20 km yields a substantially higher response than any of the other layers, for the same heating perturbations.

Randall et al. (1984) have also performed a GCM study of the response due to Saharan dust. In their experiment, the optical depth of the aerosol decreased from 1 near the West African Coast to 0 in the western Atlantic Ocean. Their study showed that a reduction occurred in the easterlies in the western Atlantic due to dust-induced heating--this is an interesting result since it is primarily the easterlies that transport dust in the first place.

Finally, with the introduction of the notion that a nuclear war or an asteroid colliding with the Earth may be accompanied by large aerosol loadings in the atmosphere (see NRC, 1985), several GCM studies have examined this climate problem. The basic climatic effects have been discussed in the "Nuclear Winter" session of the Symposium

and in Ackerman (1987). Covey et al. (1984) found that the intense radiative heating due to smoke aerosols in the aftermath of a nuclear war caused a stabilization of the midtroposphere accompanied by substantial surface cooling. They also found that meridional circulation changes caused by aerosol heating could spread the aerosols well beyond the location of the original injections. Incidentally, it is worth pointing out that changes in stability were also found by Joseph (1984) in a simulation with hypothetical large dust aerosol optical depths.

5. AEROSOL MICROPHYSICS AND TRANSPORT

All the studies mentioned above assumed fixed aerosol physical properties both in the time and space domains. Thus, microphysical processes such as coagulation, aerosol-to-cloud transformation, washout, rainout, sedimentation and Brownian diffusion were ignored in these studies. Further, the transport of aerosol away from the source regions was also not possible in these models. This inhibits a comprehensive assessment of the radiative-microphysical-dynamical interactions. In recent years, some investigations have proceeded to rectify these deficiencies by incorporating aerosol microphysical processes and by treating the aerosols as a tracer. To do this accurately is a daunting task since the range involved in describing the physical processes extends from the micrometer scale (involving aerosols) to the kilometer scale (involving large-scale transport); the task can easily overwhelm available computational resources. A few of these efforts are mentioned below. The methodologies adopted in the attempts have necessarily involved varying degrees of parameterization of the aerosol transformation and transport processes.

Newiger et al. (1984) employed the large-scale zonally averaged dynamics and cloudiness to drive the equations for aerosol microphysical processes, aerosol radiative effects, and the meridional transport. Their two-dimensional model study indicated a transport of the aerosol radiative perturbations to lower latitudes for aerosol injected initially into the middle latitudes of the Northern Hemisphere.

Westphal et al. (1987) have also performed a two-dimensional simulation of the evolution of Saharan aerosols as they are transported over desert and the eastern Atlantic in a limited area dynamical model. By comparing with observed size distributions, they concluded that the dust sizes undergo modifications during the mesoscale transport. Such a transformation implies that radiative changes would also occur during the transport.

While two-dimensional models are useful in going beyond the scope of zero- and one-dimensional models, their usefulness is limited by the use of zonally-averaged circulation statistics of the atmosphere. One way to do the more complicated three-dimensional transport

economically is to use the wind vectors from an actual GCM simulation to transport the aerosols; aerosol microphysical processes can also be treated simultaneously although feedbacks on circulation cannot be evaluated. Such modeling techniques have been pursued by Levy and Moxim (1987).

It is a natural step to make the transition to a three-dimensional GCM, which not only advects aerosols but also treats their microphysics and radiative effects explicitly and interactively. Such efforts, especially for long-term simulations, are computationally expensive so that some of the physics has to be approximated. The need for such models, however, is crucial in the investigation of the aerosol climatic effects.

One particular problem that has demanded attention to the details mentioned above is the climatic effects due to smoke aerosols in the aftermath of a nuclear war. Simulations with aerosol microphysical and interactive radiative processes have been performed in three different investigations. Malone et al. (1986) used a variation of the NCAR GCM along with aerosol absorption and bulk removal parameterizations to evaluate the smoke aerosol-induced climatic effects. The effect of introducing the aerosol removal by rain, although approximate, demonstrated that the lifetime of aerosols in the atmosphere has an important bearing on the radiative perturbations. Also, the aerosol lifetime is enhanced by reduction in convective activity, which, in turn, is initiated by the initial radiative effects. Thompson et al. (1987) have allowed for the temporal transformation of aerosol sizes, in addition to incorporating the washout and rainout processes. Their study indicates that the efficiency of removal by rain is the most important microphysical mechanism governing the radiative forcing in the middle and lower troposphere. Assumptions about aerosol optical properties were also found to be a significant factor in this study.

6. CONCLUDING COMMENTS

From the perspective of aerosol-climate interactions, the major uncertainties in the aerosol radiative forcing can be considered to arise from deficiencies in our knowledge on:

- 1) source specification and characterization of aerosol optical properties.
- 2) atmospheric effects on aerosols, and
- 3) aerosol effects on the atmosphere.

For the nominal stratospheric and tropospheric aerosols, the uncertainty in the spatial and temporal distribution of aerosol optical properties requires extensive observation networks, either ground-based or, more conveniently, through satellites. Since large perturbations in the aerosol radiative effects arise from events of an episodic nature, it will be difficult to characterize the forcing due to all such events. Examples of such events are the seasonal arctic haze and duststorms, and episodic volcanic injections. However,

observations of the evolution of aerosol derived from these sources would provide a means to ascertain the temporal evolution of the radiative forcing and to improve our understanding of transport mechanisms.

The most significant atmospheric effect on aerosols is the dry and wet removal processes in the atmosphere. Efficiency of washout and rainout of aerosols impacts directly onto the radiative effects. Parameterizations used in models require stringent testing for their mesoscale and microscale treatments such as subgrid-scale processes, cloud and precipitation formation, nucleation scavenging, etc. Cloud formation, maintenance, and dissipation, as well as transport of water in all its phases are central problems in general circulation modeling and they affect the aerosol-related issues as well. It is pointed out that current GCMs, while able to reproduce several features of the real atmosphere, possess certain deficiencies (e.g., cloud physical processes, atmosphere-ocean interactions), aspects of which impinge directly on the assessment of aerosol effects.

Aerosol-induced effects on the atmosphere involve both microphysical and radiative processes. Only the solar aspects of the latter subject has been considered in the present paper. Among the uncertainties in microphysics are the external or internal mixtures of aerosols with water drops and the dependence of this process on their physicochemical properties. Uncertainties persist in the treatment of aerosol radiative effects even if the spatial and the vertical distribution is known accurately (which, for most of the globe, is not true currently). At present, practical solutions are possible only for homogeneous and spherical aerosols, although heterogeneous and nonspherical aerosols are the rule rather than the exception. Fundamental problems concerning the light scattering by arbitrarily shaped, inhomogeneous particles require attention. Perhaps, statistical and empirical formulations (Bohren, 1986) only can provide a practical solution to this dilemma. Cloud-aerosol radiative interactions are also, indirectly, a subset of this uncertainty.

The aerosol effects on the atmosphere concern more than merely the alteration of the thermal profile. As seen from the GCM simulations, for "nominal" tropospheric aerosol forcings, radiative perturbations in the troposphere are accompanied by changes in the convective heating and in the vertical velocity. The readjustment of the energy budget by the nonradiative components in the troposphere limits the magnitude of temperature change that is predicted by the radiative and radiative-convective response assumptions. In fact, the importance of nonradiative processes in the GCM tropospheric response to a "nominal" aerosol forcing may render the search for a temperature signal in the lower troposphere, and especially at the surface, a futile task.

The GCM solutions can be quite different from the response of the more simple models that perform averaging of sorts in either the vertical or horizontal dimensions. This does not imply that the one-dimensional radiative-convective models are suited only for estimating the initial radiative forcing. They remain useful for the

analysis of the relative roles of radiative and nonradiative components in the GCM responses. The similarity between a GCM and a radiative or a radiative-convective model temperature response may exist only for the regions near or above the tropopause.

The qualitative nature of the aerosol radiative forcing on the atmosphere in terms of their absorbing and scattering properties are well understood at present. It is the quantitative determination of the quiescent and episodic aerosol radiative forcing (involving refractive indices, size distributions, vertical profiles of number densities, etc.), aspects of the microphysical forcing (e.g., changes in composition and size, with respect to space and time), and the radiative-convective-dynamical response of the atmosphere that constitute serious challenges for future investigations. For modeling efforts to be fruitful, improvements are required in the understanding and representation of physical processes and, whenever possible, in the comparison of simulations with observations.

ACKNOWLEDGMENTS

The author wishes to thank Drs. J.A. Coakley, S.B. Fels, J.D. Mahlman, and an anonymous reviewer for their constructive comments and suggestions.

REFERENCES

- Ackerman, T.P., 1987: Aerosols in climate modeling. In P. Hobbs and M.P. McCormick, (Eds.), Aerosols and Climate, A. Deepak Publishing, Hampton, VA, in press.
- Blanchet, J.P., and R. List, 1984: On Radiative Effects of the Anthropogenic Aerosol Components of the Arctic Haze and Snow in a Surface-Atmosphere Coupled Model. In G. Fiocco (Ed.), International Radiation Symposium '84: Current Problems in Atmospheric Radiation, A. Deepak Publishing, Hampton, VA, 269-273.
- Bohren, C., 1986: Review Paper on Optical Properties of Aerosols, Proceedings, Sixth Conference on Atmospheric Radiation, American Meteorological Society, Williamsburg, VA.
- Carlson, T.N., and S.G. Benjamin, 1980: Radiative Heating Rates for Saharan Dust, J. Atmos. Sci., 37, 193-213.
- Cess, R.D., G.L. Potter, S.J. Ghan and W.L. Gates, 1985: The Climatic Effects of Large Injections of Atmospheric Smoke and Dust: A Study of Climatic Feedback Mechanisms with One- and Three-Dimensional Models, J. Geophys. Res., 90, 12937-12950.
- Charlson, R.J., J.E. Lovelock, M.O. Andreae and S.G. Warren, 1987: Oceanic Phytoplankton, Atmospheric Sulfur, Cloud Albedo and Climate, Nature, 326, 655-661.
- Chylek, P., V. Ramaswamy and R. Cheng, 1984: Effect of Graphite Carbon on the Albedo of Clouds, J. Atmos. Sci., 41, 3076-3084.
- Coakley, J.A., and R.D. Cess, 1985: Response of the NCAR Community Climate Model to the Radiative Forcing by the Naturally Occurring Tropospheric Aerosol, J. Atmos. Sci., 41, 1677-1692.

- Coakley, J.A., R.D. Cess and F.B. Yurevich, 1983: The Effect of Tropospheric Aerosol on the Earth's Radiation Budget: A Parameterization for Climate Models, J. Atmos. Sci., 40, 116-138.
- Coakley, J.A., R.L. Bernstein and P.A. Durkee, 1987: Effect of Ship-Stack Effluents on Cloud Reflectivity, Science, in press.
- Covey, C., S.H. Schneider and S.L. Thompson, 1984: Global Atmospheric Effects of Massive Smoke Injections from a Nuclear War: Results from General Circulation Model Simulations, Nature, 308, 21-25.
- Deepak, A., and H.E. Gerber (Eds.), 1983: Report on the Experts Meeting on Aerosols and Their Climatic Effects, WCP-55, World Meteorological Organization, Geneva, Switzerland.
- Fels, S.B., and L.D. Kaplan, 1975: A Test of the Role of Longwave Radiative Transfer in a General Circulation Model, J. Atmos. Sci., 32, 779-789.
- Fels, S.B., J.D. Mahlman, M.D. Schwarzkopf and R.W. Sinclair, 1980: Stratospheric Sensitivity to Perturbations in Ozone and Carbon Dioxide: Radiative and Dynamical Response, J. Atmos. Sci., 37, 2265-2297.
- Fiocco, G. (Ed.), 1984: International Radiation Symposium '84: Current Problems in Atmospheric Radiation, A. Deepak Publishing, Hampton, VA, 438 pp.
- Fouquart, Y., B. Bonnel, G. Brogniez, A. Cerf; M. Chaoui, L. Smith and J.C. Vanhouette, 1984: Radiative Properties of Sahelian Aerosols. In G. Fiocco (Ed.), International Radiation Symposium '84: Current Problems in Atmospheric Radiation, A. Deepak Publishing, Hampton, VA, 71-73.
- Geleyn, J.F., and D. Tanre, 1984: Short-Term Climatic Response to the Atmospheric Aerosol Radiative Forcing. In G. Fiocco (Ed.), International Radiation Symposium '84: Current Problems in Atmospheric Radiation, A. Deepak Publishing, Hampton, VA, 243-246.
- Gerber, H.E., and A. Deepak (Eds.), 1984: Aerosols and Their Climatic Effects, A. Deepak Publishing, Hampton, VA, 297 pp.
- Grassl, H., 1987: Review paper on Radiative Effects of Atmospheric Aerosols, Aerosols and Climate Symposium, IUGG, Vancouver, Canada.
- Joseph, J.H., 1984: The Sensitivity of the Numerical Model of the Global Atmosphere to the Presence of Desert Aerosol. In H.E. Gerber and A. Deepak (Eds.), Aerosols and Their Climatic Effects, A. Deepak Publishing, Hampton, VA, 215-227.
- Levy, H., and W.J. Moxim, 1987: Fate of U.S. and Canadian Combustion Nitrogen Emissions, Nature, 328, 414-416.
- Malone, R.C., L.H. Auer, G.A. Glatzmaier, M.C. Wood and O.B. Toon, 1986: Three-Dimensional Simulations Including Interactive Transport, Scavenging and Solar Heating of Smoke, J. Geophys. Res., 91, 1039-1053.
- McClatchey, R.A., R.W. Fenn, J.E.A. Selby, F.E. Volz and J.S. Garing, 1972: Optical Properties of the Atmosphere, third ed., Rep. AFcrl-72-0497, Bedford, MA.
- Newiger, M., H. Grassl, P. Schussel and J. Rehkopf, 1984: Global Aerosol Transport and Consequences for the Radiation Budget. In G. Fiocco (Ed.), International Radiation Symposium '84: Current Problems in Atmospheric Radiation, A. Deepak Publishing, Hampton, VA, 247-251.

- National Research Council, 1985: The Effects on the Atmosphere of a Major Nuclear Exchange, National Academy Press, Washington, D.C.
- Pitari, G., M. Verdecchia and G. Visconti, 1987: A Transformed Eulerian Model to Study Possible Effects of the El Chichon Eruption on the Stratospheric Circulation, J. Geophys. Res., 92, 10961-10975.
- Pollack, J.B., and T.P. Ackerman, 1983: Possible Effects of the El Chichon Volcanic Cloud on the Radiation Budget on the Northern Tropics, Geophys. Res. Letts., 10, 1057-1060.
- Ramanathan, V., 1981: The Role of Ocean-Atmospheric Interactions in the CO₂ Climate Problem, J. Atmos. Sci., 38, 918-930.
- Ramanathan, V., and R.E. Dickinson, 1979: The Role of Stratospheric Ozone in the Zonal and Season Radiative Energy Balance of the Earth-Troposphere System, J. Atmos. Sci., 36, 1084-1104.
- Ramaswamy, V., and J.T. Kiehl, 1985: Sensitivities of the Radiative Forcing to Large Loadings of Smoke and Dust Aerosols, J. Geophys. Res., 90, 5597-5613.
- Randall, D., T. Carlson and Y. Mintz, 1984: The Sensitivity of a General Circulation Model to Saharan Dust. In H.E. Gerber and A. Deepak (Eds.), Aerosols and Their Climatic Effects, A. Deepak Publishing, Hampton, VA, 123-133.
- Shettle, E.P., and R.W. Fenn, 1979: Models for the Aerosols of the Lower Atmosphere and the Effects of Humidity Variations on Their Optical Properties, Air Force Geophysics Lab. Rep. AFGL-TR-79-0214, 94 pp.
- Tanre, D., and J.F. Geleyn, 1984: Climatic Effects Induced by the El Chichon Cloud. In G. Fiocco (Ed.), International Radiation Symposium '84: Current Problems in Atmospheric Radiation, A. Deepak Publishing, Hampton, VA, 247-251.
- Thompson, S.L., V. Ramaswamy and C. Covey, 1987: Atmospheric Effects of Nuclear War Aerosols in GCM Simulations: Influence of Smoke Optical Properties, J. Geophys. Res., 92, 10942-10960.
- Toon, O.B., and J.P. Pollack, 1976: A Global Average Aerosol Model of Atmospheric Aerosols for Radiative Transfer Calculations, J. Appl. Meteor., 15, 225-246.
- Twomey, S., 1976: Computations of the Solar Absorption of Solar Radiation in Clouds, J. Atmos. Sci., 33, 1087-1091.
- Valero, F.P., T.P. Ackerman, and W.J.Y. Gore, 1984: The Absorption of Solar Radiation by the Arctic Haze During the Haze Season and Its Effects on the Radiation Budget, Geophys. Res. Letts., 11, 465-468.
- Valero, F.P., T.P. Ackerman, and W.L. Starr, 1984: Radiative Effects of the El Chichon Volcanic Cloud. In G. Fiocco (Ed.), International Radiation Symposium '84: Current Problems in Atmospheric Radiation, A. Deepak Publishing, Hampton, VA, 144-147.
- Westphal, D., O.B. Toon and T.N. Carlson, 1987: A Two-Dimensional Numerical Investigation of the Dynamics and Microphysics of Saharan Dust Storms, J. Geophys. Res., 92, 3027-3049.